Available online at www.sciencedirect.com
SCIENCE DIRECT®
Journal of Solid State Chemistry 178 (2005) 158–165
JOURNAL OF SOLID STATE CHEMISTRY
www.elsevier.com/locate/jssc

Hydrothermal synthesis of potassium molybdenum oxide bronzes: structure-inheriting solid-state route to blue bronze and dissolution/deposition route to red bronze

Kazuo Eda[a,*], Kin Chin[a], Noriyuki Sotani[a], M. Stanley Whittingham[b]

[a]*Department of Chemistry, Faculty of Science, Kobe University, Nada-ku, Kobe 657-8501, Japan*
[b]*Institute for Materials Research, State University of New York at Binghamton, Binghamton, NY 13902-6000, USA*

Received 29 September 2004; received in revised form 28 October 2004; accepted 29 October 2004

Abstract

The hydrothermal syntheses of the alkali metal molybdenum bronzes from starting solids (H_xMoO_3) with structural affinities to the desired products were investigated. Single-phase potassium blue and red bronzes were prepared by the hydrothermal treatments at around 430 K, and characterized by powder X-ray diffraction, IR spectroscopy, and SEM. The formation processes of these two bronzes during the hydrothermal treatments were found to differ. The blue bronze was formed by a structure-inheriting solid-state route from H_xMoO_3 with $x<0.3$, whereas the red bronze was formed for $x>0.3$ through a solution dissolution/deposition route via the formation of MoO_3+MoO_2.

Keywords: Low-temperature synthesis; Hydrothermal synthesis; Potassium metal molybdenum bronze; Formation mechanism

1. Introduction

The following three types of alkali metal molybdenum bronzes are well known: (i) blue bronze, $A_{0.3}MoO_3$ with $A=$ K, Rb, Tl, and Cs [1,2]; (ii) red bronze, $A_{0.33}MoO_3$ with $A=$ Li, K, Rb, Cs, and Tl [3]; and (iii) purple bronze, $A_{0.9}Mo_6O_{17}$ with $A=$ Li, Na, K and Tl [4,5]. The structures of the blue and red bronzes have similar sheet structures consisting of clusters of ten edge-sharing MoO_6 octahedra and six edge-sharing MoO_6 octaheda, respectively, while the structure of the purple bronze consists of ReO_3-type slabs of corner-shared MoO_6 octahedra, having MoO_4 tetrahedra at the surfaces of these slabs, as shown in Fig. 1. The physical properties of the blue and purple bronzes have been extensively studied because of their charge density wave phenomenon arising from their low-dimensional metallic character [6,7]. For example blue $K_{0.30}MoO_3$ and purple $K_{0.9}Mo_6O_{17}$ show Peierls transitions at ca. 180 and 120 K, respectively. Recently, the Zawilski group reported the possible existence of a CDW in red $K_{0.33}MoO_3$ below the Peierls transition temperature of 450 K [8].

Traditionally, the alkali metal bronzes have been prepared mainly by molten salt methods at temperatures exceeding 800 K: (i) electrolytic reduction of molten mixtures of MoO_3 and A_2MoO_4, and (ii) reaction of stoichiometric mixtures of A_2MoO_4, MoO_3 and MoO_2 [7,9]. More recently some low-temperature syntheses of the bronzes have been reported [10–15].

Recently, we have focused our work on hydrothermal synthesis of alkali metal molybdenum bronzes from solids (H_xMoO_3, which is a hydrogen-insertion compound of layered MoO_3) with structural affinities to the target products [16–18]. In the present work, we could obtain single-phase potassium blue and red bronzes by the hydrothermal treatments of H_xMoO_3, and found

*Corresponding author. Fax: +81 78 503 5677.
E-mail address: eda@kobe-u.ac.jp (K. Eda).

0022-4596/$ - see front matter © 2004 Elsevier Inc. All rights reserved.
doi:10.1016/j.jssc.2004.10.043

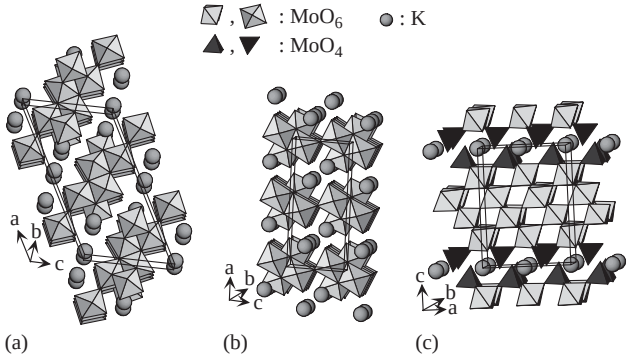

Fig. 1. Structures of alkali metal molybdenum bronzes: blue bronze (a), red bronze (b), and purple bronze (c).

that the conversion of H_xMoO_3 ($x>0.3$) during the hydrothermal reaction was quite different from that of H_xMoO_3 ($x<0.3$). According to our investigations of their conversion mechanisms, the difference was related to the presence of two types of conversion routes: one is a structure-inheriting solid-state route and the other is a solution dissolution/deposition one. Here we report the details of the hydrothermal syntheses and mechanisms of formation of the potassium molybdenum oxide bronzes.

2. Experimental

Materials preparation: The H_xMoO_3 ($0.25<x<1.34$) starting material was prepared as reported previously [19] as was the $(K\cdot nH_2O)_{0.25}[H_yMoO_3]$ (n = ca. 2) used in the present study [12,14].

Hydrothermal treatment: The starting solid suspended in 30 mL of aqueous KCl solution was placed into a 60 mL of Teflon-lined autoclave, and then heated in a forced convection oven at 431 K and autogeneous pressure. The specific solids, amounts and time are discussed in the next section. After heating, the autoclave was taken out from the oven and cooled down by an electrical fan. The resulting products were filtered, washed several times with distilled water, and dried in air.

Measurements: The powder X-ray diffraction (XRD) patterns of the samples were measured using a Mac Science MXP3VZ X-ray diffractometer with Cu$K\alpha$ radiation. Scanning electron micrograph (SEM) images of the samples were obtained in a JEOL JSM-5610LVS scanning electron microscope. The composition of the product was analyzed by a HITACHI 180-80 atomic absorption spectrometer using the 313.3 nm line for Mo, 766.5 nm line for K, and by the method of Choain and Marrion [20]. Infrared spectra were measured using a Perkin Elmer Spectrum 2000 FT-IR spectrometer.

3. Results and discussion

3.1. Products obtained by hydrothermal syntheses

Fig. 2 shows the XRD patterns of the products obtained after the hydrothermal heating of the single-phase H_xMoO_3 (1.3 g) with $x=0.25-1.34$ (mean oxidation state of Mo (M.O.S.Mo) $=5.75$–4.66) in 1.8 M KCl solution at 431 K for 48 h. The phases obtained are summarized in Table 1. According to the results, two kinds of potassium metal bronzes, blue and red bronzes, were formed in the present hydrothermal syntheses, but the purple bronze, containing tetrahedral MoO_4 units, was not obtained. There is seemingly a dividing line at M.O.S.Mo = 5.70 below which the blue bronze is formed and the red bronze is formed above it.

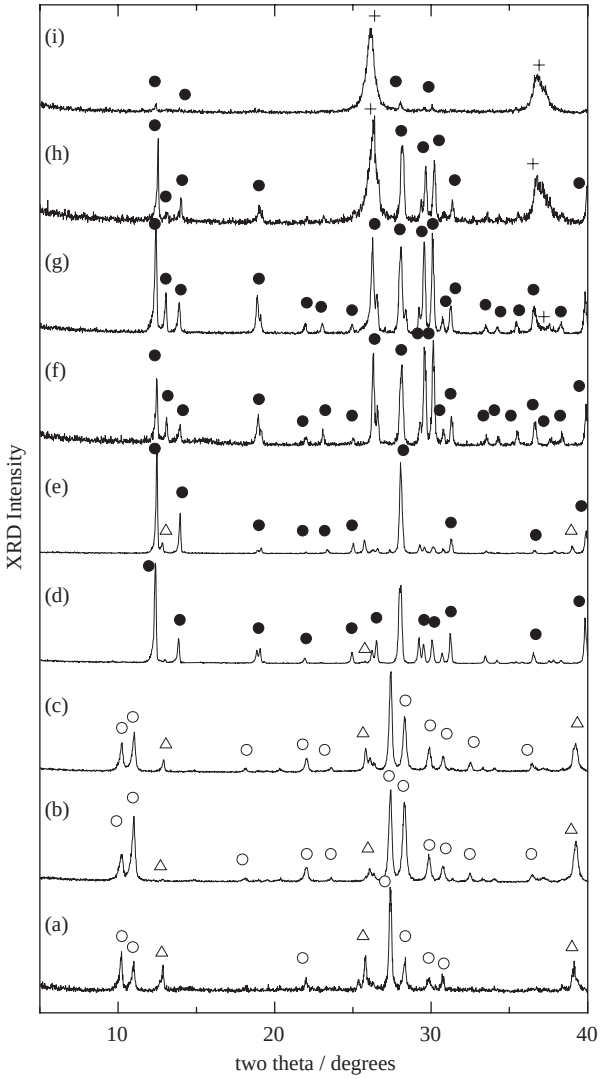

Fig. 2. XRD patterns of the products obtained by the hydrothermal treatments of H_xMoO_3 with various x values: $x=0.25$ (a), 0.28 (b), 0.29 (c), 0.30 (d), 0.31 (e), 0.36 (f), 0.47 (g), 0.91 (h), and 1.34 (i), respectively. Symbols ○, ●, △, and + indicate blue bronze, red bronze, MoO_3 and MoO_2, respectively.

Table 1
Products obtained from H_xMoO_3 with various H contents

x (M.O.S.Mo)	0.25–0.29 (5.75–5.71)	0.30–0.31 (5.70–5.69)	0.36 (5.64)	0.47–1.34 (5.53–4.66)
Products	Blue bronze + MoO_3	Red bronze + MoO_3	Red bronze	Red bronze + MoO_2

The byproducts Mo(VI)O_3 (often hexagonal decamolybdate instead of MoO_3) and Mo(IV)O_2 were formed depending on the M.O.S.Mo values of the H_xMoO_3 starting solid.

The use of lower KCl solution concentrations ($\leqslant$0.3 M KCl) or lower treatment-temperature ($\leqslant$400 K) required much longer treatment-times to obtain the bronzes. Also, when we used mixtures of MoO_3 and MoO_2 with a range of M.O.S.Mo values as starting solids instead of H_xMoO_3, we got not blue bronze, but red bronze even from the mixture with M.O.S.Mo > 5.70, unlike the case of hydrothermal treatments of H_xMoO_3. Further investigation on the hydrothermal treatments (0.43 g, in 0.9 M KCl solution at 431 K) of the MoO_3/MoO_2 mixture with M.O.S.Mo = 5.72, which was obtained by heat-treating $H_{0.28}MoO_3$ at 773 K in N_2, proved that the red bronze was formed directly from the MoO_3/MoO_2 mixture, not by way of blue bronze, as shown in Fig. 3, which shows the XRD patterns of the products formed at different stages during the hydrothermal treatment of the mixture. These results indicate product formation exhibiting a dependence on the structure (or physicochemical properties) of starting material, because the mixture of MoO_3 and MoO_2 in an environment containing abundance of water (that is, in hydrothermal aqueous solution) is regarded to be compositionally equivalent to H_xMoO_3 with a corresponding M.O.S.Mo value, which is comparable to a mixture of $(1-x/2)$ MoO_3, $x/2$ MoO_2, and $x/2$ H_2O. Such a dependence of the product on the starting material is expected to control the key elements of the structure of the product by varying the structure (or physicochemical properties) of starting solid material.

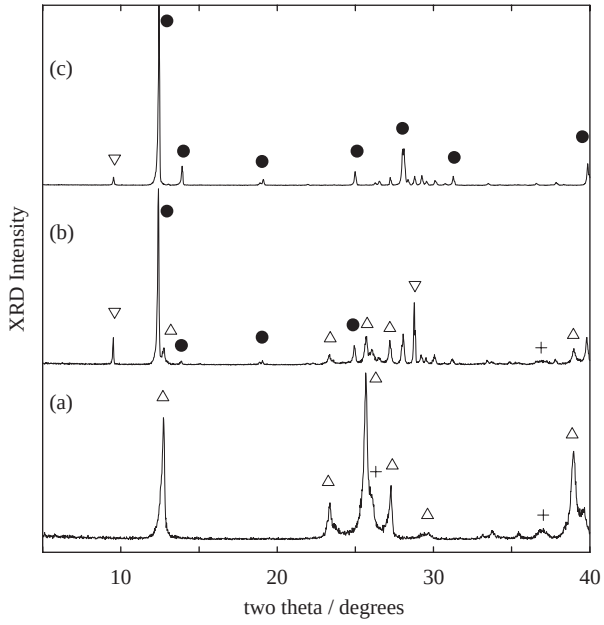

Fig. 3. XRD patterns of the products formed at various stages (various treatment-time t) during the hydrothermal treatment of the MoO_3/MoO_2 mixture, prepared by heat-treating $H_{0.28}MoO_3$ at 773 K in N_2: $t = 0\,h$ (a), 15 h (b), and 40 h (c). Symbols ●, ▽, △, and + indicate red bronze, MoO_3, hexagonal decamolybdate, and MoO_2, respectively.

3.2. Preparation and characterization of single-phase potassium metal bronzes

On the basis of the above results, we tried to obtain single-phase potassium blue and red bronzes, and succeeded in doing so. Their preparation and characterization using powder X-ray, IR, and SEM are summarized below.

3.2.1. Blue bronze

Single-phase potassium blue bronze was obtained by the hydrothermal heating of 0.43 g of $H_{0.28}MoO_3$ in 30 mL of 0.9 M deaerated KCl solution at 431 K for 48 h. In order to prevent contamination by MoO_3 or hexagonal decamolybdate, a deaerated condition was necessary for the preparation of single-phase blue potassium bronze. Loading larger amounts of $H_{0.28}MoO_3$ causes the contamination by MoO_3, as reported previously [17].

The (monoclinic) lattice constants a, b, c, and β for the single-phase blue bronze obtained were 18.283(9) Å, 7.555(5) Å, 9.864(4) Å, and 117.63(2)°, respectively, which are close to the literature data ($a = 18.249$ Å, $b = 7.560$ Å, $c = 9.855$ Å, $\beta = 117.32°$) [1]. This bronze exhibits three IR bands at 959, 946, and 911 cm^{-1} in the range 700–1300 cm^{-1}, and their frequencies agree well with the literature data [21]. The bronze sample is composed of short string-like crystallites ca. $5 \times 0.1 \times 0.1$ μm in size. The size and morphology of the crystallite did not change even after extended hydrothermal treatments. Chemical analysis gave the composition of $K_{0.28}MoO_3$ as: Calcd K 7.07 wt%, Mo 61.94 wt%, M.O.S.Mo 5.72; found K 6.90 wt%, Mo 61.50 wt%, M.O.S.Mo 5.72.

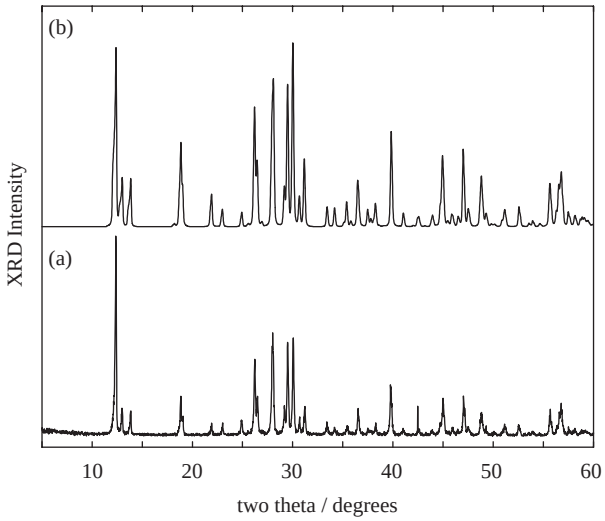

Fig. 4. XRD pattern of the potassium red bronze obtained (a) and the pattern calculated from the literature data (b).

3.2.2. Red bronze

Single-phase potassium red bronze was obtained by the hydrothermal heating of 1.3 g of $H_{0.36}MoO_3$ in 30 mL of 1.8 M KCl solution at 431 K for 30 h.

Fig. 4 shows the XRD pattern of the single-phase bronze, together with the pattern calculated from the literature data [3]. All the XRD peaks observed could be attributed to the red bronze. The (monoclinic) lattice constants a, b, c, and β of the bronze are 14.270(3) Å, 7.711(2) Å, 6.375(1) Å, and 92.61(1)°, respectively, which are close to the literature data ($a = 14.278$ Å, $b = 7.723$ Å, $c = 6.387$ Å, $\beta = 92.5°$) [3]. The chemical analysis confirmed the composition of the red bronze as $K_{0.33}MoO_3$: Calcd K 8.23 wt%, Mo 61.17 wt%, M.O.S.Mo 5.67; found K 8.11 wt%, Mo 60.76 wt%, M.O.S.Mo 5.68.

SEM images showed that the crystallites of the red bronze have a lathe-like morphology with an average size of ca. $20 \times 1 \times 0.5$ μm (Fig. 5). Extending the treatment-time resulted in even larger red bronze crystallites. This very different morphology from that of the starting $H_{0.36}MoO_3$ material suggests that the red bronze crystals have grown in the KCl solution under hydrothermal conditions.

Fig. 6 shows the infrared spectrum of the red bronze in the range 1200–700 cm^{-1}. Four peaks are observed at 968, 959, 953, and 936 cm^{-1}. These peaks are totally consistent with those measured by Hirata et al. on the red $K_{0.33}MoO_3$ powders prepared by molten method [21]. No other peaks attributed to bi-products were found in the spectrum, showing that pure phase materials can be made by this method.

3.3. Formation process of potassium metal molybdenum bronzes from H_xMoO_3

To obtain some insight into the formation processes of the potassium metal bronzes, the solid products

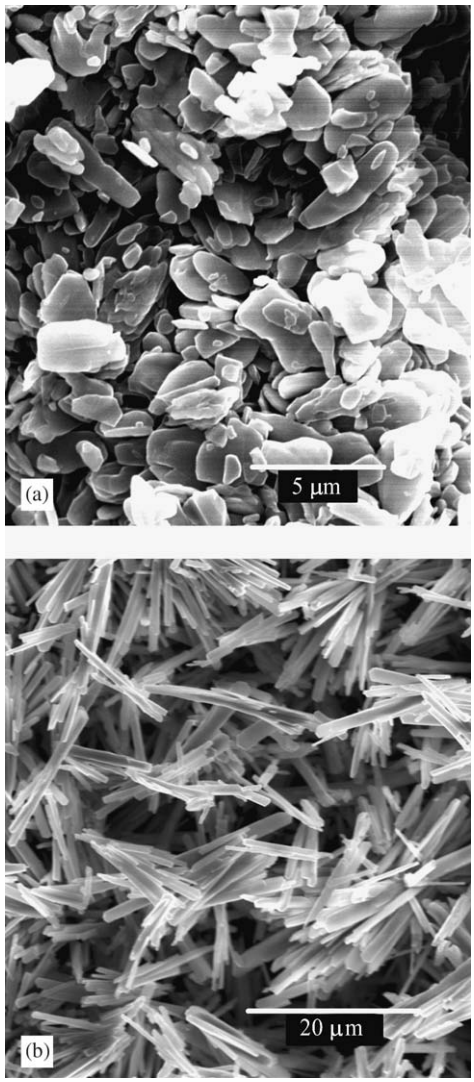

Fig. 5. SEM images of $H_{0.36}MoO_3$ (a) and the potassium red bronze obtained (b).

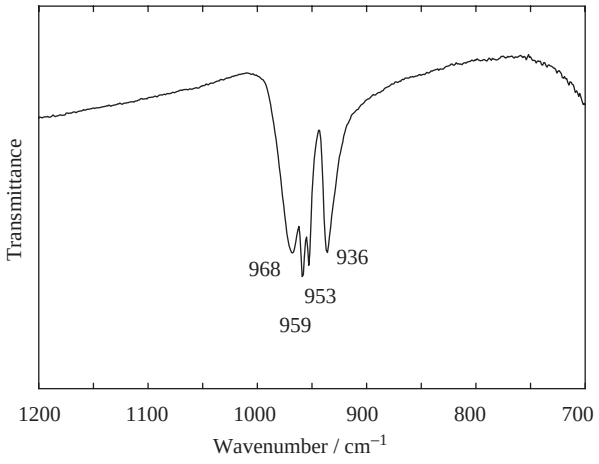

Fig. 6. IR spectrum of the potassium red bronze obtained.

formed at different stages during the hydrothermal reaction were examined by powder XRD and SEM.

3.3.1. Blue bronze

As reported previously [17], the conversion of $H_{0.28}MoO_3$ to the blue bronze during the hydrothermal reaction can be described as $H_{0.28}MoO_3 \rightarrow H_xMoO_3 +$ hydrated-type bronze $((K \cdot nH_2O)_y\ [H_{0.28-y}MoO_3)) \rightarrow$ blue bronze ($K_{0.28}MoO_3$). The topotactic insertion of hydrated K^+ ions into the interlayer region of the $H_{0.28}MoO_3$ by an ion-exchange reaction occurred, forming initially a hydrated-type bronze and then inducing a structural re-construction process leading to the formation of the potassium blue bronze [17].

According to the SEM investigations (Fig. 7), the crystallites of the blue bronze were formed by exfoliation from the surface of the crystallites of the starting solid (or the surface of crystallites of the hydrated-type bronze formed from $H_{0.28}MoO_3$ by the topotactic insertion of hydrated K^+ ions). The structural re-construction from the hydrated-type bronze to the blue bronze proceeds as a solid-state process. The fact that extended treatments did not change the morphology and size of the crystallites of the blue bronze supports the formation by a solid-state process.

3.3.2. Red bronze

Fig. 8 shows the XRD patterns of the products formed at different stages during the hydrothermal reaction of $H_{0.36}MoO_3$ (1.3 g, in 1.8 M KCl solution at 431 K). $H_{0.36}MoO_3$ also turned into hydrated-type bronze by the topotacic insertion of hydrated K^+ ions at the initial stage as in the case starting from $H_{0.28}MoO_3$ (Fig. 8b). Most of this phase, however, decomposed to MoO_3 and MoO_2 before turning into metal bronzes (Figs. 8c and d), unlike the similar hydrated-type bronze formed from $H_{0.28}MoO_3$. The red bronze was, then, formed from the MoO_3/MoO_2 mixture (Figs. 8d–g). A very small amount of blue bronze was also formed from the hydrated-type bronze, but finally disappeared. Thus, the main conversion of $H_{0.36}MoO_3$ to red bronze during the hydrothermal reaction can be described as $H_{0.36}MoO_3 \rightarrow H_xMoO_3 +$ hydrated-type bronze $((K \cdot nH_2O)_y[H_{0.36-y}MoO_3]) \rightarrow MoO_3 + MoO_2 \rightarrow$ red bronze ($K_{0.33}MoO_3$).

The SEM images showed that the crystallites of the red bronze have a larger dimension than those of the starting solid $H_{0.36}MoO_3$, indicating that they grew in the hydrothermal solution. These results suggest that the formation of the red bronze from the MoO_3/MoO_2 mixture proceeds by a dissolution/deposition process in the hydrothermal solution, that is a typical hydrothermal solution reaction. The fact that much larger crystallites of the red bronze were obtained by extending the hydrothermal treatment-time supports the formation of red bronze by a solution route.

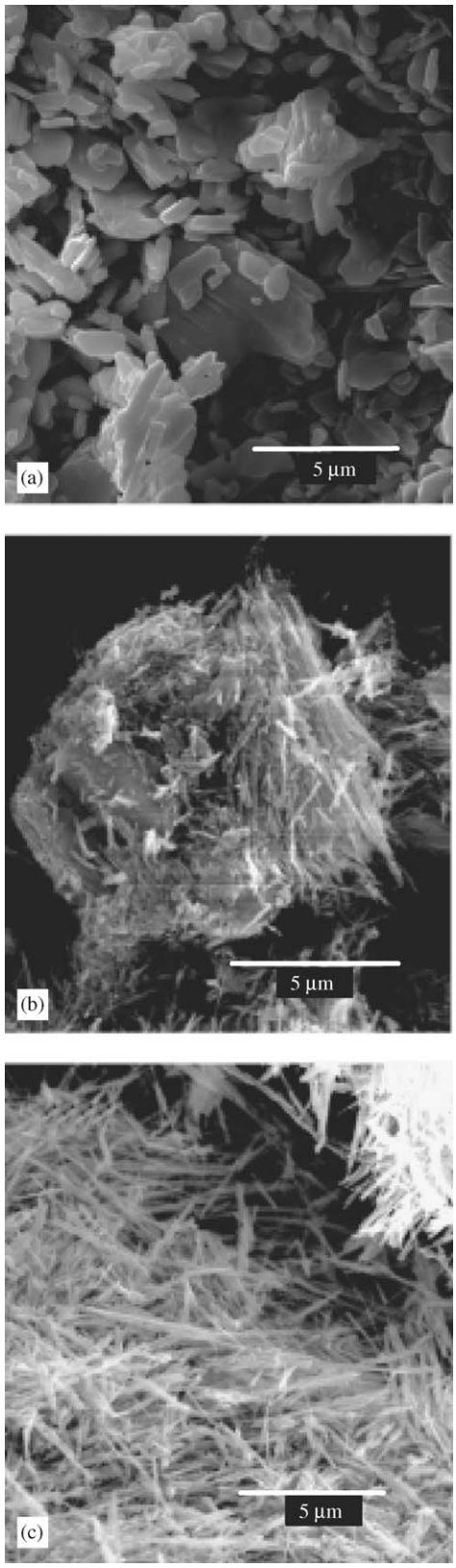

Fig. 7. SEM images of the products obtained at various stages during the hydrothermal treatment of $H_{0.28}MoO_3$: $H_{0.28}MoO_3$ as a starting solid (a), the product obtained at the stage of conversion from hydrated-type bronze to the blue bronze (b), and the blue bronze obtained as the final product.

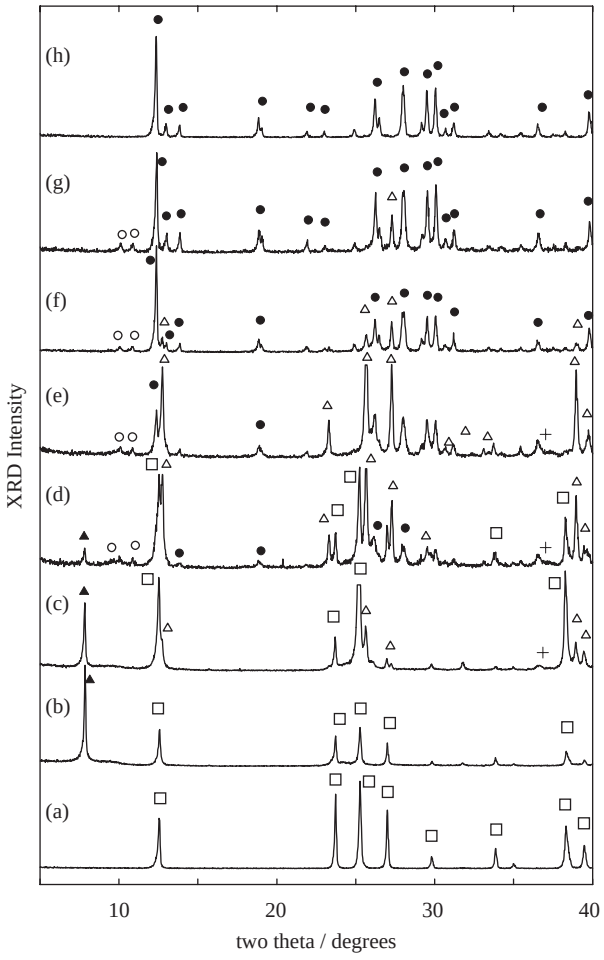

Fig. 8. XRD patterns of the products formed at various stages (various treatment-time t) during the hydrothermal treatment of $H_{0.36}MoO_3$: $t = 0$ h (a), 5 h (b), 13 h (c), 15 h (d), 15.5 h (e), 16 h (f), 17 h (g), and 18 h (h). Symbols □, ▲, △, +, ○, and ● indicate H_xMoO_3, hydrated-type bronze, MoO_3, MoO_2, blue bronze, and red bronze, respectively.

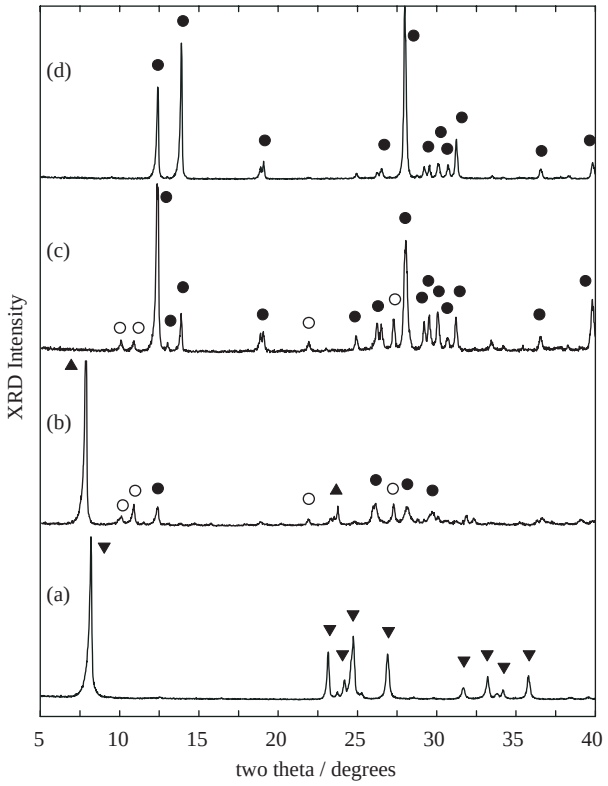

Fig. 9. XRD patterns of the products formed at various stages (various treatment-time t) during the hydrothermal treatment of the hydrated bronze $(K \cdot nH_2O)_{0.25}[H_{0.08}MoO_3]$: $t = 0$ h (a), 16 h (b), 20 h (c), and 24 h (d). Symbols ▼, ▲, ○, and ● indicate VD-type hydrated bronze, AD-type hydrated bronze, blue bronze, and red bronze, respectively.

3.4. Formation of potassium metal molybdenum bronzes from hydrated bronzes

In order to get an insight into the processes taking place during the hydrothermal formation of hydrated-type bronzes from $H_{0.28}MoO_3$ and $H_{0.36}MoO_3$, hydrothermal treatments of the hydrated bronze with well-defined compositions, $(K \cdot nH_2O)_{0.25}MoO_3$ and $(K \cdot nH_2O)_{0.25}[H_{0.08}MoO_3]$ (n = ca. 2), were investigated. The results of the former compound [17] showed that both the potassium blue and red bronzes were formed directly from the hydrated bronze with M.O.S.Mo = 5.75. The hydrated bronze did not decompose to MoO_3 and MoO_2, like the hydrated-type bronze formed from $H_{0.28}MoO_3$. The results for the hydrothermal treatments of the latter compound $(K \cdot nH_2O)_{0.25}[H_{0.08}MoO_3]$ (1.6 g, in 1.8 M KCl solution at 431 K) are shown in Fig. 9. We used as starting material vacuum-dried (VD) hydrated bronze, which has a well-defined water content; initially in the hydrothermal reaction this material takes up additional water (air-dried (AD) type bronze), just as it would on immersion in water at room temperature. All the hydrated-type bronzes formed during the hydrothermal treatments of H_xMoO_3 were AD-type bronzes. This hydrated bronze with M.O.S.Mo = 5.67 gave an almost pure single phase of the potassium red bronze. The transient formation of a very small amount of blue bronze was also observed. These results agree well with the results of the hydrothermal treatment of $H_{0.36}MoO_3$. However, in this case there was no evidence of the intermediate formation of MoO_3 and MoO_2, unlike the hydrated-type bronze formed from $H_{0.36}MoO_3$ (Fig. 8). This result suggests that the red bronze might also be formed directly from the hydrated-type bronze via a solid-state process and not just from the MoO_3/MoO_2 mixture. Our SEM investigation, however, did not give any evidence such as retention of morphology to support the solid-state process for the formation of red bronze, although the possibility still remains.

These differences in reaction behavior, during the hydrothermal treatments, between the hydrated-type bronzes formed from $H_{0.28}MoO_3$ or $H_{0.36}MoO_3$ and the

hydrated bronzes, $(K \cdot nH_2O)_{0.25}MoO_3$ and $(K \cdot nH_2O)_{0.25}[H_{0.08}MoO_3]$, whose interlayer K^+ sites are fully occupied might be related to differing chemical compositions. That is, the former have a lower K content (or a higher H content) than the latter. However, the hydrated-type bronzes could not be separated from the resultant mixtures obtained in the hydrothermal treatment and therefore could not analyze their compositions. Therefore, in order to get insight into these differences, we investigated the stability under hydrothermal conditions of $H_{0.28}MoO_3$ and $H_{0.36}MoO_3$ having higher H contents than the hydrated bronzes, and these results are described below.

3.5. Structural stability of H_xMoO_3 under hydrothermal condition

Fig. 10 shows the XRD patterns of the products formed at different stages during the hydrothermal treatment of $H_{0.28}MoO_3$ and $H_{0.36}MoO_3$ (1.3 g) in distilled water at 431 K. After the 16 h hydrothermal treatment, $H_{0.36}MoO_3$ has completely decomposed to MoO_3 and MoO_2, while $H_{0.28}MoO_3$ essentially retained its hydrogen bronze structure. Even after a 36 h treatment, $H_{0.28}MoO_3$ still retained the hydrogen bronze structure to some extent. Thus, $H_{0.36}MoO_3$ decomposes much quicker than $H_{0.28}MoO_3$, which originates from some unstablizing factor such as its higher hydrogen activity or lower Mo oxidation state. It is reasonable that the hydrogen thermodynamic activity increases with increasing hydrogen content, thus potentially making $H_{0.36}MoO_3$ unstable. According to these results, it is reasonable that the hydrated bronzes, $(K \cdot nH_2O)_{0.25}MoO_3$ and $(K \cdot nH_2O)_{0.25}[H_{0.08}MoO_3]$ with a lower H content, did not decompose to MoO_3 and MoO_2 under hydrothermal conditions. In contrast, it is suggested that the hydrated-type bronze formed during the hydrothermal treatments of H_xMoO_3, especially the hydrated-type bronze from $H_{0.36}MoO_3$, has a higher H content (or a lower K content), and does decompose.

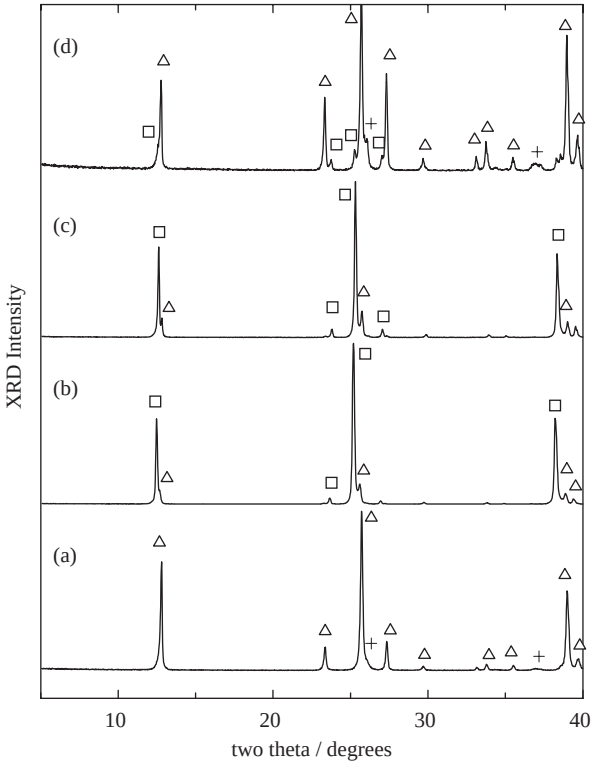

Fig. 10. XRD patterns of the products obtained after hydrothermal treatments of $H_{0.36}MoO_3$ and $H_{0.28}MoO_3$ in water: 16 h treatment of $H_{0.36}MoO_3$ (a), 16 h treatment of $H_{0.28}MoO_3$ (b), 22 h treatment of $H_{0.28}MoO_3$ (c), and 36 h treatment of $H_{0.28}MoO_3$ (d). Symbols △, +, and □ indicate MoO_3, MoO_2, and H_xMoO_3, respectively.

3.6. Two types of formation routes in the hydrothermal syntheses of potassium bronzes

Thus, there are two types of formation routes in the hydrothermal syntheses of potassium metal bronzes: one is a solid-state route and the other is a solution dissolution/deposition route.

Potassium blue bronze is formed only from hydrated (or hydrated-type) bronzes through the solid-state route. The schematic of the formation of single-phase blue bronze during the hydrothermal treatment of $H_{0.28}MoO_3$ is depicted in Fig. 11. The structures of both the starting solid, $H_{0.28}MoO_3$, and the product, blue bronze, are constructed of similar infinite zigzag chains of edge-sharing MoO_6 octahedra, and there is a strong structural affinity between them. Further, the topotactic insertion of hydrated K^+ cation into $H_{0.28}MoO_3$ by an ion-exchange reaction gives the starting solid a compositional affinity to the bronze. The resulting intermediate product, a hydrated-type bronze, turns into the blue bronze through a solid-state structural re-construction. Consequently the product, blue bronze, partially inherits the structure of the starting solid, $H_{0.28}MoO_3$, and we refer to the whole route from $H_{0.28}MoO_3$ to the blue bronze as a structure-inheriting solid-state route.

In the hydrothermal treatment of $H_{0.36}MoO_3$, (with M.O.S.Mo < 5.70) a hydrated-type bronze with a higher

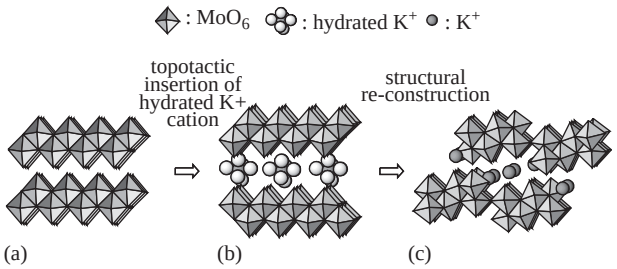

Fig. 11. The formation processes from $H_{0.28}MoO_3$ to the blue bronze: $H_{0.28}MoO_3$ (a), hydrated-type bronze (b), and the blue bronze (c).

H content might be expected to form, which decomposes to MoO_3 and MoO_2 before the potassium molybdenum oxide bronzes can be formed through the structure-inheriting solid-state route. Thus, the potassium red bronze is formed mainly from the MoO_3/MoO_2 mixture via a solution route, although there is the possibility that it is formed directly from hydrated (or hydrated-type) bronzes in the solid-state route if the kinetics over-ride the thermodynamic decomposition reaction. In support of this mechanism, the red bronze can be formed from MoO_3/MoO_2 mixtures, where it must proceed in solution because of the lack of similarity between the structures of MoO_3 and MoO_2, and the red bronze.

4. Conclusions

Single-phase potassium blue and red potassium molybdenum bronzes have been synthesized at an extremely low temperature (around 430 K) by the hydrothermal treatment of H_xMoO_3. These single-phase bronzes were characterized by powder XRD, IR spectroscopy, and SEM investigation. These studies showed that the two bronzes were formed by different routes. The blue bronze is formed by a structure-inheriting solid-state route, whereas the red bronze is formed through a solution dissolution/deposition route. By using the former structural-inheriting route, the key elements of the structure of the products can be controlled by varying the structure of the starting solid; however, the matrix of the solid must be stable under the reaction conditions.

References

[1] J. Graham, A.D. Wadsley, Acta Crystallogr. 20 (1966) 93.
[2] K. Eda, T. Miyazaki, F. Hatayama, N. Sotani, J. Solid State Chem. 137 (1998) 12.
[3] N.C. Stephenson, A.D. Wadsley, Acta Crystallogr. 18 (1965) 241.
[4] M. Onoda, K. Toriumi, Y. Matsuda, M. Sato, J. Solid State Chem. 66 (1987) 163.
[5] M. Onoda, Y. Matsuda, M. Sato, J. Solid State Chem. 69 (1987) 67.
[6] M. Greenblatt, Chem. Rev. 88 (1988) 31.
[7] A. Manthiram, Rev. Inorg. Chem. 6 (1984) 1.
[8] B. Zawilski, J. Richard, J. Marcus, Solid State Commun. 109 (1999) 41.
[9] A. Wold, W. Kunnmann, R.J. Arnott, A. Ferretti, Inorg. Chem. 3 (1964) 545.
[10] K. Eda, K. Furusawa, F. Hatayama, S. Takagi, N. Sotani, Bull. Chem. Soc. Jpn. 64 (1991) 161.
[11] C. Tsang, A. Dananjay, J. Kim, A. Manthiram, Inorg. Chem. 35 (1996) 504.
[12] N. Sotani, T. Suzuki, K. Eda, M. Yanagi-ishi, S. Takagi, J. Solid State Chem. 132 (1997) 330.
[13] C.F. Tsang, A. Manthiram, J. Mater. Chem. 7 (1997) 1003.
[14] N. Sotani, T. Manago, T. Suzuki, K. Eda, J. Solid State Chem. 159 (2001) 87.
[15] K. Eda, Chem. Lett. (2001) 74.
[16] K. Eda, K. Chin, M. S. Whittingham, Chem. Lett. (1999) 811.
[17] K. Chin, K. Eda, N. Sotani, M.S. Whittingham, J. Solid State Chem. 164 (2002) 81.
[18] K. Chin, K. Eda, T. Suzuki, N. Sotani, Bull. Chem. Soc. Jpn. 76 (2003) 557.
[19] N. Sotani, K. Eda, M. Sadamatsu, S. Takagi, Bull. Chem. Soc. Jpn. 62 (1989) 903.
[20] C. Choain, F. Marion, Bull. Soc. Chim. Fr. (1963) 212.
[21] T. Hirata, K. Yagisawa, J. Phys.: Condens. Matter 2 (1990) 5199.